

# APPROXIMATE TRAVELLING DISTANCES OF WATER MIST DROPLETS IN TUNNELS

*Richard Crosfield, Angelo Cavallo, Francesco Colella,  
Ricky Carvel, José L. Torero & Guillermo Rein  
BRE Centre for Fire Safety Engineering, University of Edinburgh, UK*

## ABSTRACT

The small droplets used in water mist systems can be transported long distances by the tunnel longitudinal ventilation flow. This paper investigates the problem using a simple model of droplet aerodynamics to calculate the landing distances under different ventilation flows and conditions common in modern tunnels. The problem is simplified by considering a single droplet falling from the tunnel ceiling and reaching the road deck. Random unimodal spatial turbulence is included in the model and the expression for the drag coefficient is calibrated against experimental results of falling droplets in a small tunnel 0.3 m in diameter and 6 m long. The results from this simple model provide for small droplets very good agreement (less than 2.3 % difference) with CFD code Fluent calculations in a 3D domain using RANS turbulence modelling. The results for the scenario of a modern tunnel with  $3 \text{ m}\cdot\text{s}^{-1}$  ventilation flow show that most water mist droplets, those less than  $170 \mu\text{m}$ , are carried between 60 and 130 m downstream before they reach the deck, and 130 and 750 m for flow of  $10 \text{ m}\cdot\text{s}^{-1}$ . A significant proportion of the water mist is carried away for very large distances for similar or larger ventilation velocities. According to these results, the zone lengths for the water mist systems should be considerably longer than the 50 m long stipulated by the World Road Association (PIARC) for flows up to  $10 \text{ m}\cdot\text{s}^{-1}$ . An alternative strategy, in order to reduce the lengths of nozzle zone, would be to reduce the ventilation flow during the water mist response.

## 1. INTRODUCTION

At present, there is a significant interest in water based suppression systems for tunnel infrastructures. The emphasis, particularly in Europe, seems to be on water mist systems rather than traditional sprinkler systems. Water mist systems are being installed in a number of tunnels in Austria, Spain (Madrid M30 ring road), France (Paris A86 ring road) and Russia (Moscow, Silver Forest). Other road tunnel operators are considering the use of such systems in their existing facilities.

What distinguishes a water mist system from other sprinkler systems is the much smaller size of the droplets. A water mist is a spray for which approximately 90% of the total volume corresponds to droplets of less than  $500 \mu\text{m}$  in diameter [1, 2]. Most current commercial systems for tunnel applications provide droplet diameters in the range 30 to  $170 \mu\text{m}$ . By comparison, a conventional sprinkler produces droplet diameters of the order of  $1000 \mu\text{m}$ . These fine mist droplets have a high surface to volume ratio and carry very little momentum (very low terminal velocity). Using smaller droplets in suppression systems has several practical advantages, not least the fact that such systems use much lower water flows, and hence require smaller pipes and

smaller reservoirs to feed them. This reduces the cost and weight of the system, compared to sprinklers, and is therefore more attractive for very long tunnels.

The high surface to volume ratio enhances the heat transfer from the flame and hot gases to the mist. The momentum of mist droplets is low enough for them to circulate around obstructions - acting like a total flooding gas – and (it is claimed) reaching into covered locations such as the motor compartments and passenger compartments of vehicles. However, one major disadvantage is that mist droplets can easily be blown away from the fire location by fire-induced flows, natural wind and the tunnel ventilation.

In the 2008 PIARC document on fixed fire-fighting systems [3], it is proposed that one of the requirements of a fixed fire-fighting system is that it must “be designed to handle air velocities in the range of  $10 \text{ m}\cdot\text{s}^{-1}$  that can result from ventilation system operation or natural effects”. The implication of this statement is that a suppression system should be designed to operate with the ventilation system running at maximum capacity. However, given the size of the small droplets, it is likely that most of the mist would be blown away from the incident location and it seems highly unlikely that the system would be near the optimum operating conditions in such large ventilation flows.

The problems associated with the use of water mist systems in tunnels are not trivial. The mechanisms leading to the control of a fire by water mists are complex and poorly understood. There are very few fundamental studies in this area, and most of the work focuses on the assessment of performance via large scale tests. To the best knowledge of the authors, no experiments have addressed the landing distance of water mist droplets in tunnels under higher ventilation conditions.

This paper studies the transport of droplets in tunnels using a simple model of droplet aerodynamics and focuses on the landing distances for different longitudinal ventilation conditions. The predictions from the simple analytical model are compared to the prediction of a commercial Computational Fluid Dynamics (CFD) package and the result of experiments conducted in a small tunnel.

## **2. DROPLET DIAMETERS IN COMMERCIAL SYSTEMS**

As part of this study, a number of water mist manufacturers were consulted and the approximate droplet size distributions in their systems were obtained. Droplet sizes from 35 to 300  $\mu\text{m}$  are found to be characteristic of these current commercial systems for tunnels. The following is an approximation of the size distribution.

- 35  $\mu\text{m}$  – Droplets of this diameter are significantly smaller than the average size and represent the lower bound diameter. These droplets will result in the upper bound for landing distances.
- 90 and 120  $\mu\text{m}$  – This range may be taken to represent the average droplet diameter of current systems.
- 170  $\mu\text{m}$  – This diameter is significantly larger than the average size and may therefore be considered to represent the upper bound. These droplets will result in the lower bound

for landing distances.

- 300  $\mu\text{m}$  – This value is well above the upper bound of droplet diameters, but is also included as an indication of travel distances of very large droplets (*e.g.* possible coalesced droplets).

### 3. THE NEED FOR DROPLET TRAJECTORY ASSESMENT

Detailed CFD modelling of a water mist system could provide, in principle, some useful information on the delivery of water to the fire [4]. However, CFD simulations alone are not the best first approximation to a complex problem, like the one being studied here, when more fundamental studies have not been tried yet and when experiments are not available. This first attempt to address the problem moves away from full CFD but is intentionally simple, transparent and easy to validate. It is intended that further mechanisms and complexity can be built upon this foundation in the future.

Water mist systems commonly use a zonal strategy; the system is subdivided into a number of zones of a given length, and only those zones closest to the fire are activated in the event of a fire. In a tunnel with longitudinal flow, a commonly adopted strategy would be to activate two zones; the zone containing the fire itself and the zone upstream of the fire location. In order for this strategy to be useful, the zone must be of sufficient length that the prevailing ventilation does not carry the droplets beyond the fire location. See Figure 1.

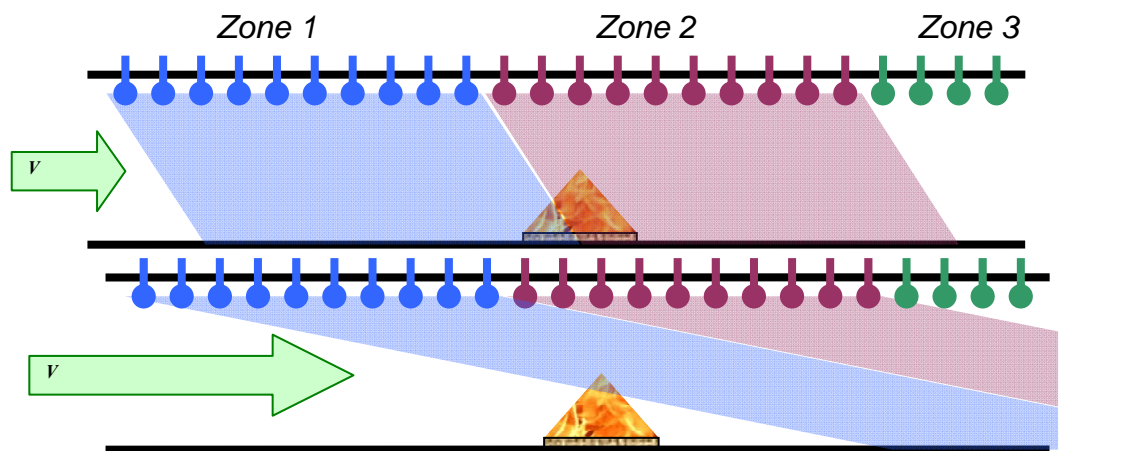


Figure 1. Top) A water mist system that reaches the fire location for a given longitudinal ventilation. Bottom) A water mist system that misses the fire location at higher longitudinal ventilation

Figure 1 shows at the top a scenario where the ventilation is sufficiently low and the zones are sufficiently long that the mist generated in both Zone 1, upstream of the fire, and Zone 2, at the fire location is able to reach the fire location. In the scenario shown at the bottom of Figure 1, the ventilation is such that all the droplets from Zone 1, upstream of the fire, (and Zone 2) are carried beyond the fire location before they reach road level. If ventilation rates of this magnitude are to be considered, Zone 1 must be much longer than pictured (*i.e.* extend much further upstream) in order for any droplets from Zone 1 to be able to attack the fire itself.

#### 4. MODEL OF DROPLET AERODYNAMICS

An analytical model of droplet transport aerodynamics has been developed. This is a simple model, merely intended to provide a rough estimate of the travel distances and provide an assessment of the performance of water mist systems under specific conditions. The flow is assumed to be cold (*i.e.* no fire conditions) and the droplet is inert and does not evaporate.

The model calculates the movement of a droplet of diameter  $d$  moving at velocity  $\mathbf{V}$  on the vertical centre plane of the tunnel, under gravitational pull  $\mathbf{g}$  and a longitudinal flow  $\mathbf{U}$ . The droplet is injected at the ceiling height  $H$  with a given injection spray velocity  $V_s$  and at angle  $\theta_s$  with the ceiling. Figure 2 is a representation of the scenario under consideration. The droplet is carried along by the airflow as it falls and ultimately impacts on the road deck at some downstream distance  $L_d$  from the nozzle location.

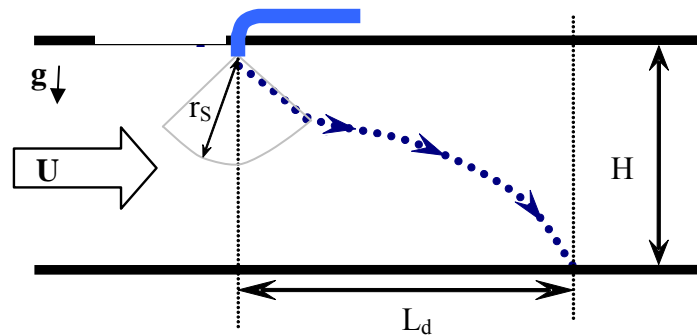


Figure 2. Trajectories of water mist droplets in a horizontal tunnel. As a droplet exits the spray-momentum cone, it is carried along by the ventilation airflow and ultimately impacts on the road deck.

The conservation of momentum in vector notation considering inertia, gravity and drag leads to Eq. (1) for the expression of the droplet acceleration.

$$\frac{\partial \mathbf{V}}{\partial t} = \mathbf{g} + \frac{1}{2} C_D \frac{\rho A_d}{m} \|\mathbf{W}\| \mathbf{W} \quad (1)$$

Where  $\mathbf{g}$  is the gravity vector;  $C_D$  the drag coefficient for a sphere is given by Eq. (2) [5];  $\rho$  the air density;  $A_d$  the projected area of the droplet;  $m$  the mass of the droplet; and  $\mathbf{W}$  the droplet velocity vector relative to the ventilation flow and given by Eq. (3). Integration in time of Eq. (1) with the given initial conditions provides the trajectory of the droplet.

$$C_D^i = 0.4 + \frac{24}{Re} + \frac{6}{1 + \sqrt{Re}} \quad (2)$$

$$\mathbf{W} = \mathbf{U} - \mathbf{V} \quad (3)$$

The Reynolds number  $Re$  in the drag coefficient (Eq. (2)) is calculated using the relative droplet velocity and given by Eq. (4), where  $\nu$  is the air kinematic viscosity.

$$\text{Re} = \frac{d\|\mathbf{W}\|}{2\nu} \quad (4)$$

Near the injection point, there is a cloud of conical shape with the apex at the nozzle, where the mist is dense and the momentum injected by the spray dominates the droplets movement. While a droplet is inside this nozzle cone, its trajectory is a straight line following the initial spray angle and moving at the injection spray velocity. Typical nozzle cones for water mist applications can stretch to vertical distances  $r_s$  in the range of 1 to 2 m from the nozzle. See Figure 2. In this simple model it is assumed that there is no interaction between the prevailing flow and the droplets in the cone, this is a conservative assumption. For certain nozzle and injection pressure configurations it is likely that the droplets will reach terminal velocity with regard to the flow in considerably smaller distances.

Outside the nozzle cone, the fine droplets experience a large drag force relative to both the gravitational force, and rapidly reach falling terminal velocity (which is in the range  $0.1$  to  $0.4 \text{ m}\cdot\text{s}^{-1}$  for the droplet sizes considered here). The droplets are then carried along by the airflow. Only the droplet injected along the downstream edge of the spray is considered here as this will be the one landing the furthest downstream.

Two main limitations exist for this model that stem from the assumptions of an isolated droplet and no fire-induced heating or flow. The falling trajectory is calculated here assuming an isolated droplet once it is away from the nozzle (out of the momentum-dominated nozzle cone). This assumes that there is no interaction with other droplets, which is valid for sparse water mists (*i.e.* low water flow rates or large tunnel sections). The addition of the fire into the problem will produce even finer droplets due to evaporation together with an upward lift and enhanced turbulence from the buoyant plume. However, these two effects are of lesser importance than large ventilation flows and would tend to result in larger transport distances than those calculated here.

## 5. RESULTS FOR AVERAGE FLOW CONDITIONS

The first analysis carried out [6] did not include the effect of turbulence, but only considers a uniform and constant horizontal flow. Thus it provides the mean path of many droplets that would be falling under perturbed flow conditions. The longitudinal flow in the tunnel  $\mathbf{U}$  is modelled as a parabolic velocity profile (zero velocity at the ceiling and deck and maximum value at the centre) with an average flow velocity  $U_0$

$$U_x = 8U_0 \left[ \left( \frac{y}{H} \right) - \left( \frac{y}{H} \right)^2 \right] \quad (5)$$

$$U_y = 0$$

where  $U_x$  and  $U_y$  are the horizontal and vertical components, respectively, of the velocity; and  $y$  is the vertical distance from the road deck. This profile is characteristic of fully developed laminar flow in pipes.

The trajectories have been calculated for a range of ventilation velocities  $U_0$  up to  $10 \text{ m}\cdot\text{s}^{-1}$ . The tunnel ceiling height  $H$  is 6 m, the spray velocity  $V_s$  is  $10 \text{ m}\cdot\text{s}^{-1}$ , spray angle with the ceiling  $\theta_s$  is  $25^\circ$ , and the nozzle cone size  $r_s$  is 2 m. Figure 3 shows that the landing distance for droplet diameters and ventilation flows of interest in commercial systems span from 10 m to 900 m.

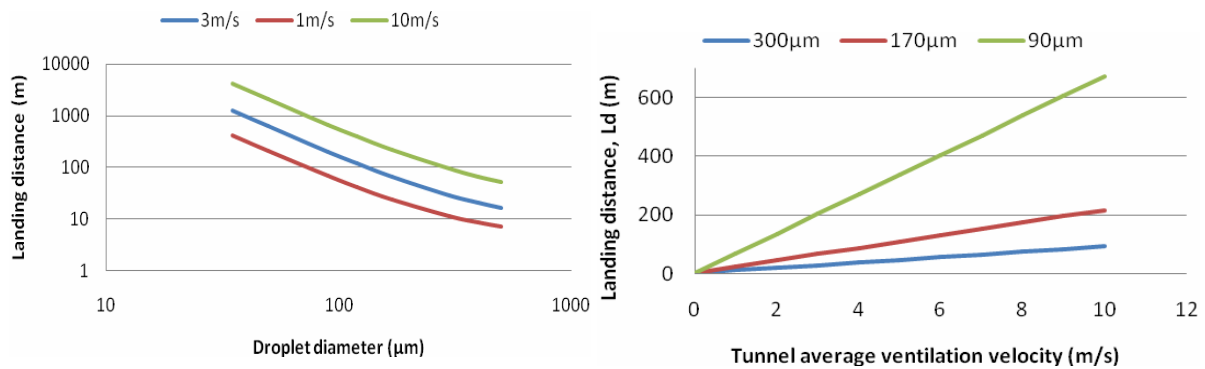


Figure 3. Landing distances (left) vs. diameter; and (left) vs. airflow velocity for droplets ejected at a ceiling height of 6 m Note the logarithmic scale in the left plot.

Figure 4 shows the landing distance vs. the spray injection velocity and angle for a droplet diameter of  $300 \mu\text{m}$  (well above the upper bound diameter in commercial systems) and an average flow of  $3 \text{ m}\cdot\text{s}^{-1}$ . The landing distance only increases from 21 to 29 m for a wide range of injection velocity from 0 to  $10 \text{ m}\cdot\text{s}^{-1}$ . It decreases from 33 to 20 m with the spray angle from horizontal to  $90^\circ$  and then increases to 22 m as droplets are injected in the opposite direction to the ventilation flow when  $\theta_s > 90^\circ$ .

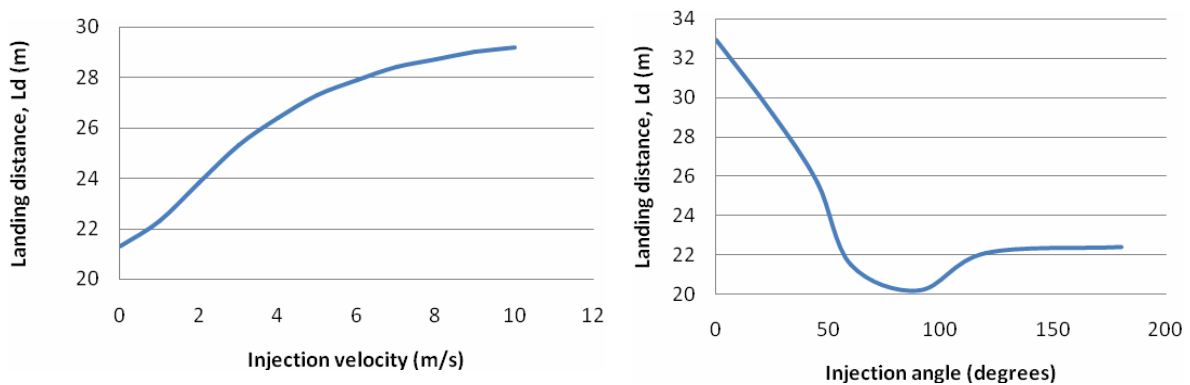


Figure 4. Sensitivity of the landing distance vs. injection velocity (left) and vs. injection angle (right) for a  $300 \mu\text{m}$  diameter droplet ejected at a ceiling height of 6 m under a horizontal average flow of  $3 \text{ m}\cdot\text{s}^{-1}$ .

Figure 5 shows results of the landing distance vs. the spray cone length and vs. the tunnel height (i.e. injection height) for a droplet diameter of  $300 \mu\text{m}$  and an average flow of  $3 \text{ m}\cdot\text{s}^{-1}$ . The distance is reduced from 31 to 22 m when the cone height varies from 0 to 4 m (in a tunnel 6 m high). The distance increases linearly with the tunnel height.

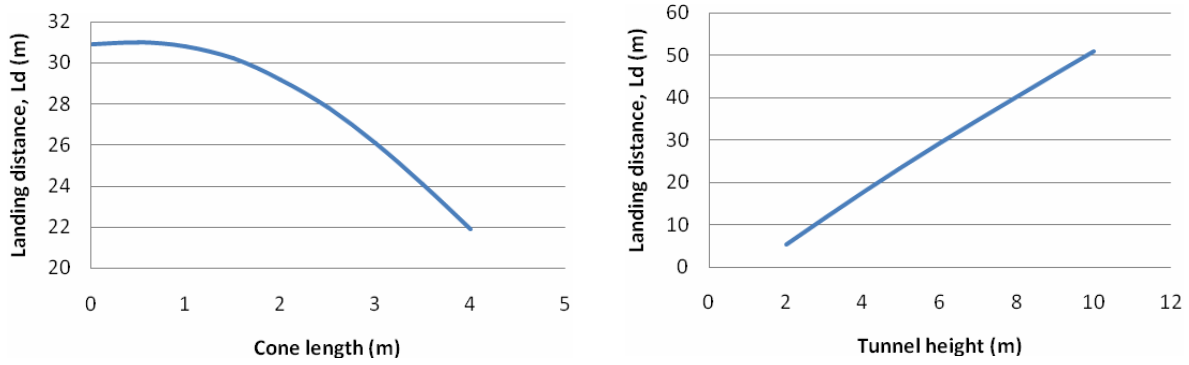


Figure 5. Sensitivity of the landing distance vs. cone length when ejected at a ceiling height of 6 m (left) and vs. tunnel height (right) for a 300 μm diameter droplet under a horizontal average flow of 3 m·s<sup>-1</sup>.

The results indicate that the landing distance does not depend strongly on the parameters of the spray (injection velocity, angle and cone length) that lead to less than 30% reduction over a very wide range of possible spray operating conditions. Only the tunnel height has a large impact on the results, as it is to be expected.

## 6. RESULTS IN TURBULENT CONDITIONS

The effect of turbulence was modelled by the addition of perturbations to the parabolic flow profile (Eq. (5)) used for the laminar case. Random perturbations of different intensities are generated in the horizontal and the vertical components of the velocity using Eq. (6).

$$\begin{aligned}
 U_x &= 8U_0 \left[ \left( \frac{y}{H} \right) - \left( \frac{y}{H} \right)^2 \right] + U_0 I_x \Omega_1 \sin(2\pi \Omega_2 k y) \\
 U_y &= U_0 I_y \Omega_3 \sin(2\pi \Omega_4 k y)
 \end{aligned}
 \tag{6}$$

where  $\Omega_i$  is a random number,  $k$  is the wavenumber, and  $I_x$  and  $I_y$  are the turbulence intensities in the horizontal and vertical directions respectively. The turbulent intensity is defined as the ratio of the root-mean-square of the velocity fluctuation to the mean horizontal velocity  $U_0$ . For a fully-developed flow, the horizontal turbulent intensity is given by empirical correlations to be between 1% and 15% [7]. In particular, for a modern tunnel (6 m high and flows from 1 to 10 m·s<sup>-1</sup>), the Reynolds number is between 10<sup>4</sup> and 10<sup>7</sup>, which results in turbulent intensities between 2 and 3.5% [7]. The most appropriate wavenumber  $k$  for this application can be determined using the approximation that the ratio of eddy size  $\ell$  to tunnel height is approximately 0.07 for fully-developed turbulent flow in pipes [7]. Since one period of the wave is equivalent to two eddies, the following expression is reached for  $k$ :

$$k = \frac{1}{2\ell} \approx \frac{1}{2 \cdot 0.07H} \approx \frac{7}{H}
 \tag{7}$$

A unique turbulent velocity profile is generated for each drop using the random numbers  $\Omega_i$

(generated between -1 and 1). This allows for a Monte Carlo-type of approach to study the distribution of trajectories from a large population of droplets. Figure 6 shows the histogram and reconstructed density functions of the results.

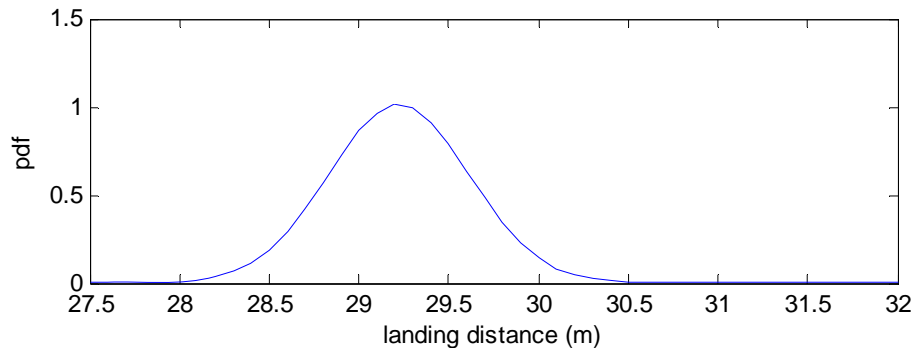


Figure 6. Probability density function of predicted landing distances under a turbulence intensity of  $I_x = 20\%$  and  $I_y = 0$  for a  $300\ \mu\text{m}$  diameter droplet under a horizontal average flow of  $3\ \text{m}\cdot\text{s}^{-1}$ . Results for  $k = 7/H$  and a population of 100 droplets.

Figure 7 shows results of the landing distance vs. the turbulence intensities.

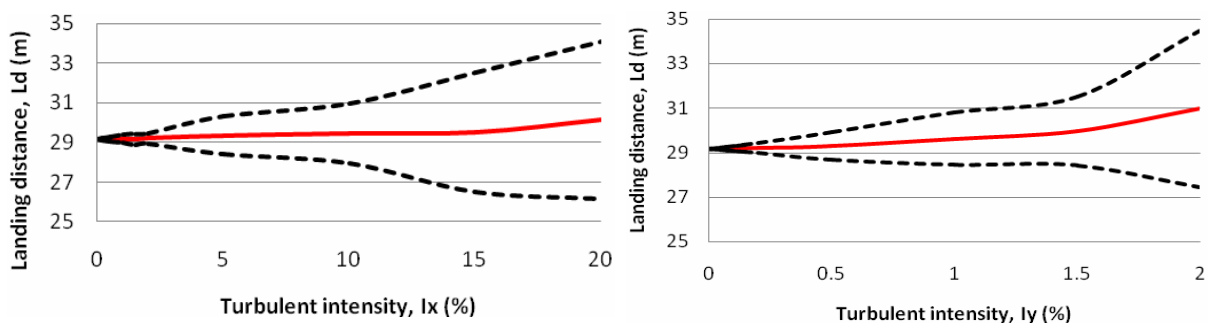


Figure 7. Sensitivity of the landing distance; (left) vs. horizontal turbulent intensity (and no vertical turbulence); (right) vs. vertical turbulent intensity (and no horizontal turbulence). Results are for  $k = 7/H$  and a population of 100 droplets. The red solid line is the mean landing distance and the dashed lines are the maximum and the minimum values predicted in the population.

The mean distance remains fairly constant in the range 29 to 31 m. Only the range between maximum and minimum distances increases significantly with turbulence (up to  $\pm 6$  m in the case of large turbulence). The vertical intensity is more influential in relative terms than the horizontal, but this is a product of the definition since both are calculated as a percentage of the mean horizontal velocity  $U_0$ , which is much larger than the vertical fluctuations (mean of zero). Because of this low sensitivity, upper bound values are chosen as worst case scenarios for turbulence, and for subsequent simulations the horizontal intensity is fixed at 20% and the vertical one at 5%. The sensitivity to wavenumber values is low as well (results not shown), with landing distance of  $29 \pm 2$  m at low wavenumber ( $k \approx 1/H$ , large eddies) and decreasing to  $29.5 \pm 0.5$  m for high wavenumber ( $k \approx 14/H$ , small eddies).

## 7. COMPARISON WITH EXPERIMENTS AND CFD

A small tunnel was constructed to test the validity of the model predictions. All four sides walls where made of transparent PMMA and had a square 0.3 m side cross-section and a length of 6 m. A fan with maximum capacity for  $1800 \text{ m}^3 \cdot \text{h}^{-1}$  and a speed controller provided average ventilation velocities in the range of  $2$  to  $5 \text{ m} \cdot \text{s}^{-1}$ . A honeycomb box was introduced immediately downstream of the fan in order to shorten the flow entrance length to 5 m. The flow profile was measured at several points along the tunnel to assure the droplets where injected at a test section with fully developed flow conditions. Droplets were generated using a syringe. Because the smallest syringe in the market is of  $0.15 \text{ mm}$  inner diameter, the smallest droplets that could be generated were of  $1.8 \text{ mm}$  diameter. Between 60 and 70 dyed droplets were injected with zero initial velocity and at an angle of  $90^\circ$  with the ceiling. Their landing distances were recorded by measuring the horizontal distance between the nozzle and the marks left by the dye on graph paper on the tunnel deck. Figure 8 (left) shows the distribution for landing distances obtained for one test. For a flow of  $4.8 \text{ m} \cdot \text{s}^{-1}$ , the mean distance is  $174 \text{ mm}$  and the standard deviation is  $12 \text{ m}$  (7%).

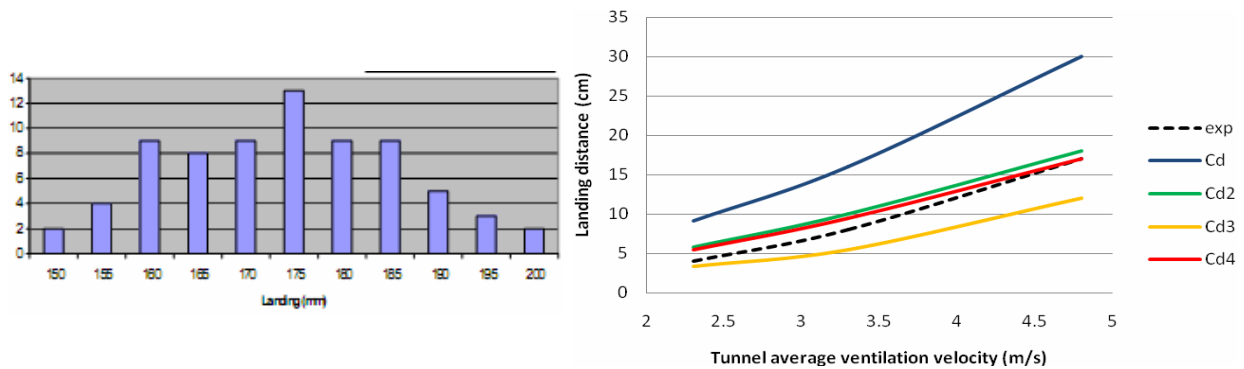


Figure 8. (left) Histogram of measured landing distances for an average flow of  $4.8 \text{ m} \cdot \text{s}^{-1}$ ; and (right) comparison of experimental measurements and model predictions using the different drag coefficients.

The experimental results were used to calibrate the drag coefficient expression used in the mathematical model. The literature provides a variety of expressions for the drag coefficients in travelling droplets. For the range of droplet Reynolds number of interest here (between 40 and 200), four expressions have been found in the literature; the basic one,  $C_D^i$ , for a sphere given in Eq. (2) [5] and those particular to a water droplet,  $C_D^{ii}$ ,  $C_D^{iii}$  and  $C_D^{iv}$  given by in Eqs. (8-10) [8, 9 and 10 respectively]:

$$C_D^{ii} = \frac{24}{\text{Re}} \left( 1 + \frac{\text{Re}^{2/3}}{6} \right) \quad (8)$$

$$C_D^{iii} = 0.133 \left( 1 + \frac{150}{\text{Re}} \right)^{1.565} + 4I_x \quad (9)$$

$$C_D^{iv} = \frac{24}{\text{Re}} (1 + 0.1935 \text{Re}^{0.6305}) \quad (10)$$

Figure 8 (left) compares the experimental results with the analytical model predictions using

different drag coefficients. The experimental values lie within the range predicted using expressions for  $C_D^{iii}$  and  $C_D^{iv}$ , and closer to the later. The results using  $C_D^i$  are too high (around 80%), and the result using  $C_D^{ii}$  are close to those with  $C_D^{iv}$ . Thus, the drag coefficient for  $C_D^{iv}$  was selected as the most appropriate for calculating the transport of water droplets in duct flows.

Despite the very good agreement with the experiments, these were conducted in a small tunnel with relatively big droplets (too big to be mist droplets). Thus, to extrapolate the validation of the results to mist droplets and more realistic conditions (6 m high tunnel and droplet diameters in the 100  $\mu\text{m}$  range), CFD simulations are used.

Using the commercial code Fluent CFD, an isolated droplet in a in a 3D tunnel was simulated under the same spray and ventilation conditions as discussed above. A Lagrangian method is used to track the movement of an inert particle using the k- $\epsilon$  model for RANS turbulence under fully-developed periodic flow imposed by periodic flow boundary conditions. The CFD model is able to predict the experimental results in the small tunnel within 5% error (results not shown). The results for a 6 m tunnel are shown in Table 1, together with comparison of the analytical model predictions.

The comparison is very positive for the analytical model since results differ by only 0.1 to 2.3% in the range of droplet diameters of interest for water mists (below 300  $\mu\text{m}$ ). The difference is smaller for larger ventilation velocities. For droplets larger than 500  $\mu\text{m}$ , the difference is significant and rises up to 19 to 36%. Considering the much larger computational resources and solution time required for the CFD runs, the supports the use of the simple analytical model to study this problem.

More complex CFD scenarios, including the spray formation, multiple droplets and multiple nozzles are possible, but are only justified after the analytical model has been used to provide full understand of the basic transport mechanisms. This is to avoid unnecessary complexity. The main drawback from model of large complexity is the potential black-box effect. This happens when the modelling is not providing understanding of the processes at hand but only predictions of a complex process, sometime intractable predictions. This effect might lead to mere numerical fitting of results instead of physical modelling.

The only results found in the literature on landing distances are from one of the simulations provided as part of the large CFD study of water mist systems in tunnels for fire [4]. The CFD simulation of the turbulent aerodynamics of a  $1 \text{ kg}\cdot\text{s}^{-1}$  mist from a realistic spray nozzle and the full interactions between droplets and a ventilation of  $2.4 \text{ m}\cdot\text{s}^{-1}$ , in a tunnel 3 m high, provided a mean landing distance of 12 m for the cloud of 120  $\mu\text{m}$  diameter droplets. This result can be compared to our simple scenario of an isolated inert droplet under the same spray and ventilation conditions using the analytical model, which provides a landing distance of 14 m. This 16% difference is remarkable given the simplicity a one droplet scenario compared to the full spray model.

H =6 m, $V_s=10 \text{ m}\cdot\text{s}^{-1}$ , $\theta_s=90^\circ$								
	$U_0=3 \text{ m}\cdot\text{s}^{-1}$				$U_0=5 \text{ m}\cdot\text{s}^{-1}$			
d ( $\mu\text{m}$ )	1000	500	300	100	1000	500	300	100
$L_d$ (m) CFD	5.5	11.8	21.8	96.5	9.7	20.5	35	-
$L_d$ (m) Analytical	7.5	12.9	21.3	96.6	11.5	21.2	35.5	161
Difference	36%	9%	-2.3%	-0.1%	19%	3.4%	1.4%	

Table 1. Comparison of analytical model predictions and CFD predictions. The analytical model used  $C_D^{iv}$  as the drag coefficient, and values of 20% and 5% for the horizontal and vertical turbulence intensity respectively.

## 8. IMPACT OF PIARC'S RECOMENDATIONS

After validation of the model in the range of interest, it is applied in this section to asses the impact of the recommendation by PIARC (use of water mist systems under ventilations velocity up to  $10 \text{ m}\cdot\text{s}^{-1}$ ). Figure 9 shows. The effect of the nozzle cone can be observed in the first 2 m of trajectory.

The results show that water mist droplets from 90 to 170  $\mu\text{m}$  in diameter , the great majority of the droplets in commercial tunnel water mists systems, are carried between 60 and 130 m downstream before they reach the road deck in a tunnel with only  $3 \text{ m}\cdot\text{s}^{-1}$  airflow. A minority of the droplets, those larger 300  $\mu\text{m}$  will be carried less than 20 m downstream under  $3 \text{ m}\cdot\text{s}^{-1}$  airflow. For a flow of  $10 \text{ m}\cdot\text{s}^{-1}$ , droplets from 90 to 170  $\mu\text{m}$  in diameter will land between 130 and 750 m downstream of the nozzle. Even the biggest droplet of 300  $\mu\text{m}$  will and between 60 and 90 m away for  $10 \text{ m}\cdot\text{s}^{-1}$ .

The results shown above predict that individual droplets (or sparse mists of droplets which do not interact significantly with each other) may be carried hundreds of metres downstream of the nozzle location before hitting the road deck under ventilation conditions that are commonplace in tunnels. Thus, if the current ventilation strategies are to be employed in the event of a fire, the zone length should be considerably longer than 50 m, especially if droplets smaller than 170  $\mu\text{m}$  are being used (as is generally the case). Zone length in the order of 400 m would seems more appropriate but would results in excessively expensive suppression systems.

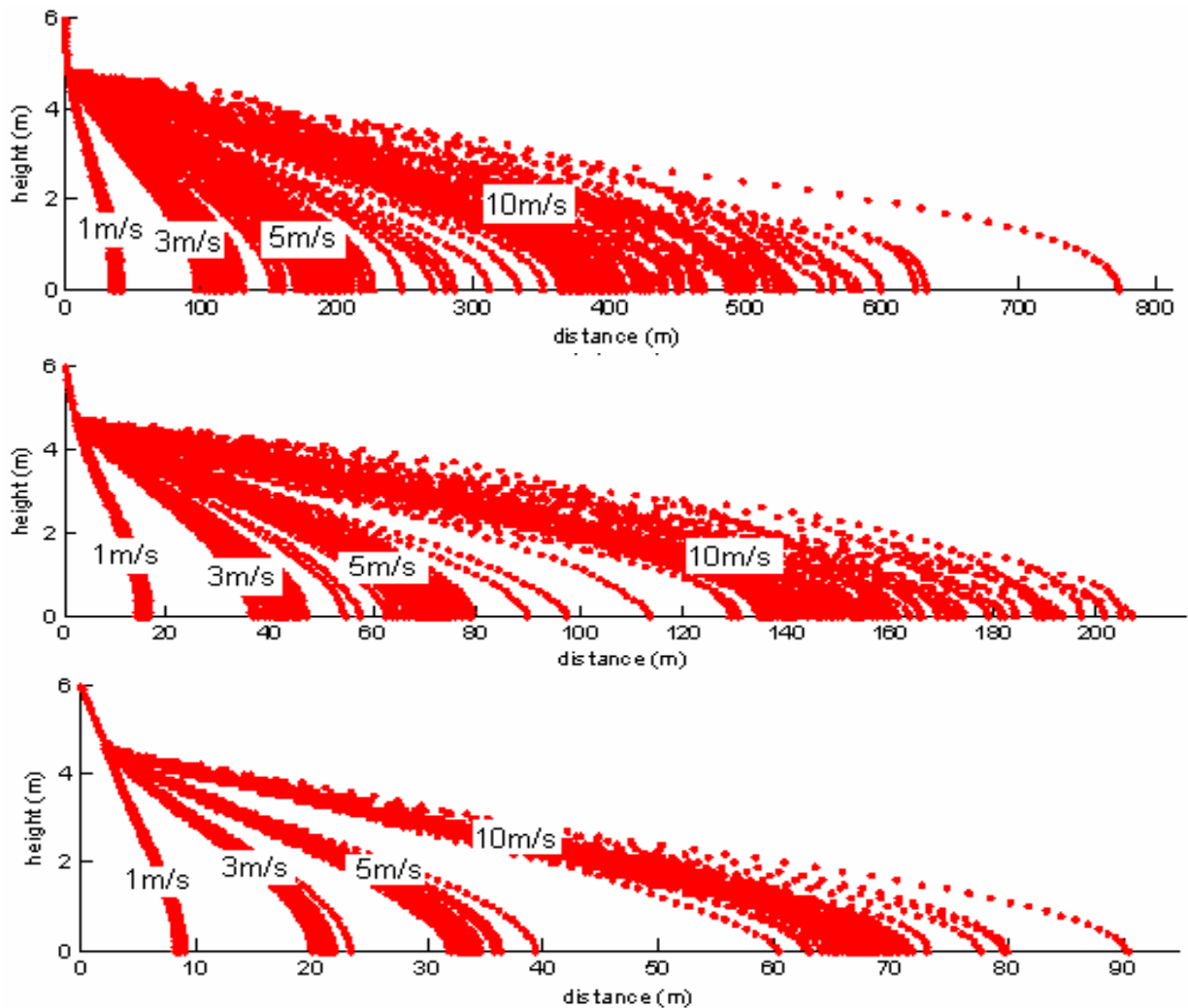


Figure 9. Landing distances for droplet of diameter; (top)  $90\ \mu\text{m}$ , (middle)  $170\ \mu\text{m}$  and (bottom)  $300\ \mu\text{m}$  in a horizontal tunnel section, subject to average longitudinal airflows of 1, 3, 5 and  $10\ \text{m}\cdot\text{s}^{-1}$ .  $C_D^{iv}$  was used as the drag coefficient, and values of 20% and 5% for the horizontal and vertical turbulence intensity respectively.

An alternative strategy, in order to reduce the lengths of nozzle zone and increase mist effectiveness, would be to reduce the ventilation flow during emergency response. This appears to be contrary to the recommendations of PIARC, quoted above, and is a non-trivial procedure that will require a thorough analysis of the flows within any tunnel, before implementation. The upper limit of ventilation rate under which a water mist system may be useable needs to be assessed for each commercially available water mist system, bearing in mind that buoyant flow in sloping tunnels can significantly increase longitudinal airflow.

## 9. CONCLUDING COMMENTS

Combining the results of this study with the implications of the wording of the PIARC document quoted above [3] would suggest that water mist systems are not fully appropriate for tunnel fire safety applications. Yet water mists are increasingly being installed in tunnels without revision of

the zone lengths.

Perhaps the issue needs to be addressed in a systemic manner. Rather than trying to design a water mist system to operate in conjunction with an independent ventilation system, the system should be rather designed as unified one, consisting of two subsystems, water mist and ventilation. While the optimum operating conditions, if such exist, for the unified water mist and ventilation system is unknown at this point, it seems unlikely that this will be at maximum ventilation. The model and results presented here could be applied towards this design.

## **ACKNOWLEDGEMENTS**

Thanks to Marioff, Fogtec, Jacobs Engineering (UK) and Prof. Andre Marshall (University of Maryland) for interesting discussions on the topic.

## **REFERENCES**

1. Grant, G., Brenton, J., Drysdale, D., Fire suppression by water sprays, *Progress in Energy and Combustion Science* 26, 79-130, 2000.
2. Gagnon, R. M. *Design of Water-Based Fire Protection Systems*. Delmar Publishers, Albany, New York.
3. PIARC Technical Committee C3.3, *Road Tunnels: An Assessment of Fixed Fire Fighting Systems*, Report 2008R07, ISBN: 2-84060-208-3, 2008, [www.piarc.org](http://www.piarc.org)
4. Hart, R. A., *Numerical Modelling of Tunnel Fire and Water Mist Suppression*, PhD Thesis, University of Nottingham, 2005.
5. White, F.M., *Viscous Fluid Flow*, McGraw-Hill, New York, 1974.
6. G. Rein, R.O. Carvel, J.L. Torero, *Study of the Approximate Trajectories of Droplets from Water Suppression Systems in Tunnels*, 3rd International Symposium on Tunnel Safety and Security, Stockholm, Mar. 2008. pp. 141-148.
7. Versteeg, H.K., Malalasekera, W, *An Introduction to Computational Fluid Dynamics. The Finite Volume Method*, 2nd ed., Pearson Education Ltd., England, 2007.
8. Rudinger, G., *Fundamentals of Gas-Particle Flow*, *Handbook of Power Technology*, Elsevier, 1980.
9. Uhlherr, P. H. T., Sinclair, C. G., *Proc. of chemeca '70*. 1, 1-13, Butterworths of Australia, Melbourne, 1970.
10. Clift, R., Grace, J. R., Weber, M. E., *Bubbles, Drops and Particles*, Academic Press, 1978.